Macromolecular Entanglement. IV. Modulus of Swelling Acrylic Fibers as a Means of Studying Macromolecular Entanglements

B. QIAN,* J. ZHU, J. HE, P. HU, and C. WU

Man-Made Fiber Research Institute, China Textile University, Shanghai, 200051, China

SYNOPSIS

In a swelling state at a temperature of incipient dissolution, an acrylic fiber is highly elastic just like a rubber. A system of entangled macromolecular chains is considered analogous to a cross-linked rubber network and from the theory of rubber elasticity, the measured extension modulus of an acrylic fiber at the terminal swelling state may be used to calculate the number of entanglements. By means of a capillary rheometer, a series of model acrylic fibers with varied degrees of entanglements were prepared. The entanglements present in these model fibers were then measured by the other two thermal methods (SDSC and SSS/SS methods) already established in our laboratory. The die swell ratios were also measured microscopically at the exit of the capillary rheometer. The experimental results of entanglements measured by the various methods were well correlated, at least qualitatively.

INTRODUCTION

When a material is strained, a stress will be generated in the material. The strain can be of various types, for example, extension, compression, or shear; the stress also has various types. The ratio of stress to strain is called a modulus. For a viscoelastic polymer, like plastics, rubber, or fiber, the stress–strain relation is usually nonlinear when the strain is rather big and the modulus depends much upon time and temperature.

According to whether the stress is alternate or constant, the modulus may be termed dynamic or static. The different types of dynamic modulus are summarized by Ferry.[1]

The modulus of fibers tested for this article is static. The change of modulus of the fiber with temperature is in general a reflection of the change of fiber texture, sometimes termed supermolecular structure. The texture is stabilized by intermolecular bonds and loosened by macromolecular mobility, both dependent upon temperature. If the fiber is immersed in a solvent that is a fiber swelling agent, the curve relating the modulus of the swelling fiber with progressively rising temperature will be more sensitive than when the fiber is unswollen, from which much textural information of the swelling fiber can be obtained.

* To whom correspondence should be addressed.

Journal of Applied Polymer Science, Vol. 53, 1261–1275 (1994)
 CCC 0021-8995/94/101261-15

EXPERIMENTAL

Instrumentation

The instrument used in our laboratory for determining the thermomechanical properties of fibers was a self-designed and constructed thermomechanical analyzer for fibers of the type TMA XRF-2.[2] An automatic electronic analytical balance was employed as a force measuring device. The fiber sample can be immersed in a swelling agent, usually an 80% aqueous dimethyl formamide (DMF) solution for acrylic fibers. A variety of thermomechanical tests can be made with the self-recording TMA instrument when the fiber is subjected to a programmed temperature rise:

1. a thermal shrinkage test with the fiber sample subjected to a small constant stress or

2. a thermal shrinking stress test with the fiber sample kept at constant length.

The results of the above two tests for an ultrahigh molecular weight polyacrylonitrile (UHMWPAN) fiber sample are shown in Figure 1(a,b).

3. During a thermal shrinking stress test run at a rather low heating rate of about 1°C/min, the heating program may be temporarily interrupted at a certain temperature and the sample allowed to shrink several tenths of a millimeter to several millimeters, then the stress on the shrinking stress–temperature curve experiences a sudden drop of a certain magnitude. The corresponding shrinkage of the fiber can be read from a digital display provided on the instrument. The shrinking modulus of the fiber at this temperature can then be easily calculated from the ratio of shrinking stress drop to the corresponding shrinkage. The results of the above tests are shown in Figure 2(a–c).
4. The TMA XRF-2 instrument was also used to determine the load–elongation properties of a swelling fiber at a series of temperatures, and the corresponding moduli of the fiber sample was then calculated. The result of such a measurement is shown by a typical example given below.

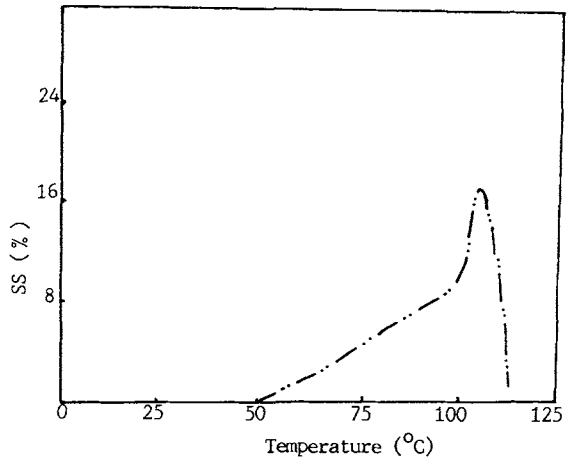

Figure 1(a) Thermal swelling shrinkage (SS) curve of an UHMWPAN fiber, subjected to a small constant stress of 0.9 mg/dtex (1 mg/d), immersed in a swelling agent of 80% aqueous DMF (sample: single filament of 4.23 dtex (3.81 d); $\bar{M}_w = 120 \times 10^4$, draw ratio = 4). *Note:* Denier (d) is a unit of fiber fineness usually employed in textile circles. It is the weight of 9000 m of the fiber. A more rational unit is the tex which is the weight of 1000 m of the fiber. Decitex (dtex) is even a more convenient unit. The weight is expressed in grams.

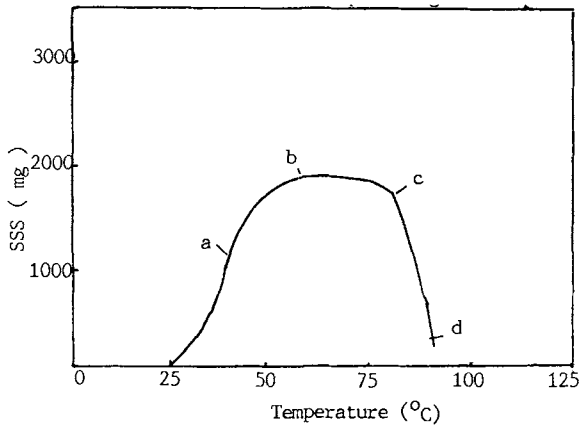

Figure 1(b) Thermal swelling shrinking stress (SSS) curve of an UHMWPAN fiber [same as Fig. 1(a)], kept at a constant length [SSS(max) = 425 mg/dtex].

Thermomechanical Analytical Data as a Means of Characterizing Fiber Texture

Temperature-Shrinking Stress and Shrinkage Curves

It is obvious that the temperature–shrinking stress and shrinkage curves for swelling and unswollen fibers are closely related to the fiber texture. Partic-

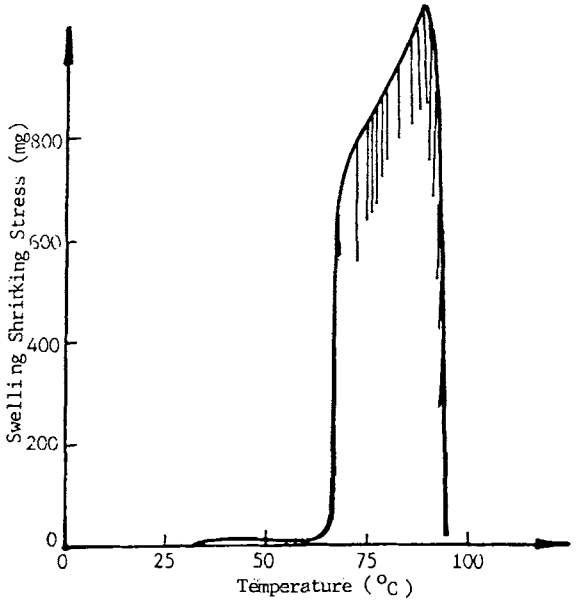

Figure 2(a) Determination of swelling shrinking modulus during thermal swelling shrinking stress test at a heating rate 1°C/min. Sample: PAC fibers produced by Jingshan Jinglun Plant; 10 filaments with total titer of 33.3 dtex; swelling agent: 80% aqueous DMF. l_0 = 40.23 mm; Δl(mm): 0.06, 0.30, 0.30, 0.76, 1.20, 1.40, 1.42, 1.52, 2.14, 1.73, 2.00, 2.40, 2.54, 2.51, 2.50, 3.06, where l_0 is the initial length of the sample and Δl the length changes adopted at various temperatures; the corresponding changes of the shrinking stress are shown in the curve.

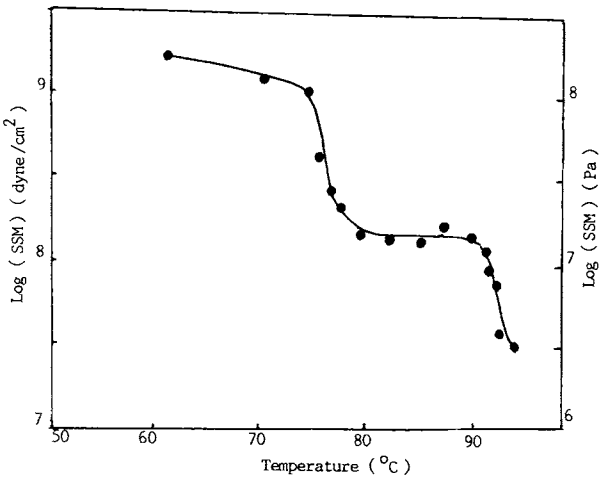

Figure 2(b) Temperature–swelling shrinking modulus (SSM) curve as determined from Figure 2(a).

ularly, the ratio of maximum swelling shrinking stress (SSS) to maximum swelling shrinkage (SS), designated as R (SSS/SS), has been proved to be a measure of macromolecular entanglement.[3]

Temperature–Modulus Curve and Texture

It is well known that the temperature–modulus curve of a polyacrylonitrile copolymer (PAC) fiber is characterized by several zones: glassy, leathery, crystalline (plateau), melting, and terminal.

The demarcation of the temperature–modulus curve into the various zones remains essentially the same when the sample is immersed in a solvent although the detail of the curve, particularly the corresponding temperature zones, may be somewhat different.[4]

Referring to Figure 2(c) the modulus–temperature curve of a swelling PAC fiber begins by a short flat portion before point, "a," corresponding to the glassy zone with a modulus of about 10^8 Pa (10 dyne/cm^2 = 1 Pa). Following rising temperature, the curve (ab) turns rapidly downward. In this region, the material becomes pliable or leathery corresponding to the leathery zone. In the following plateau zone, the modulus changes slightly; the texture in the plateau zone (bc) is mainly determined by the chain network in which the existing crystallites acting as cross-links are only slowly attacked by the swelling solvent under this temperature range. With a further rise in temperature, a point, c, is reached where the crystalline texture is rapidly dissociated. The cd zone corresponds to the melting zone of the fiber. The final stage after d is termed the terminal swelling state when all the crystalline texture is destroyed. For a short interval of further temperature rise, only entanglement loopings are left

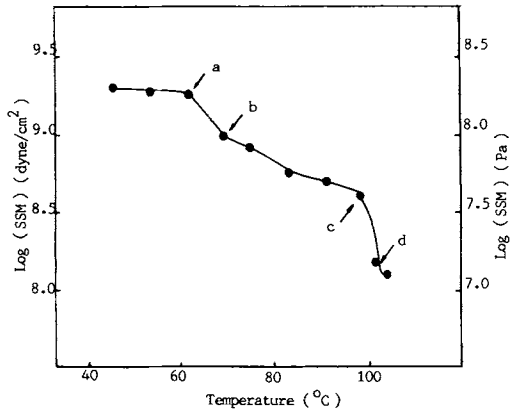

Figure 2(c) Temperature–swelling shrinking modulus (SSM) curve of an UHMWPAN fiber (same as Fig. 1), using a similar test process as Figure 2(a,b).

in the texture and thereafter the fiber will be completely dissolved.

At the state of incipient dissolution, d, we accidently took the sample out of the instrument, and we found that the swelling fiber sample still existed there between the clamps. To our great astonishment, the swelling fiber can be rapidly extended by several hundred percent and still retract instantly to its original unstretched state. It behaves exactly like a rubber. No doubt, the fiber is now a highly

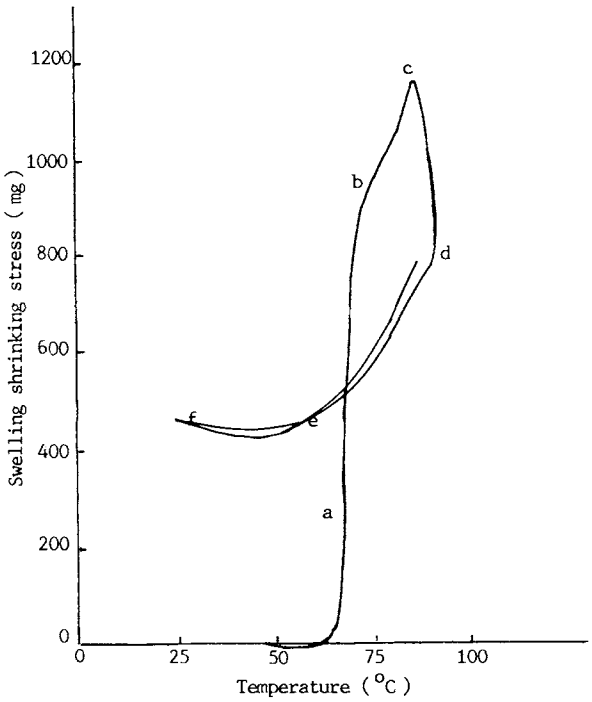

Figure 3 Attainment of the terminal swelling state of a PAC fiber by repeated heating and cooling during thermal shrinking test (sample: PAC fiber bundle, $\bar{M}_w$ = 6 × 10^4, 51.1 dtex/20 filaments; draw ratio = 11).

swollen network (a gel) with very few crystallites left as network cross-links but nearly the whole macromolecular entanglements or loopings still remain intact.

For the purpose of complete dissociation of all texture of the fiber except the macromolecular entanglements, we let the swelling sample at the temperature of incipient dissolution (*d* in Fig. 3) cool down once again to below 40–50°C and the shrinking stress was recorded down as usual (see Fig. 3). All through the process, the length of the fiber sample was kept constant. The swelling fiber sample was then reheated to the point d of incipient dissolution. By this thermal cycle, all remnant textural units in the swelling fiber were eliminated, leaving a network structure with macromolecular entanglements as cross-links, which fits a rubber model very closely. The temperature–shrinking stress record of a PAC fiber during the first heating, cooling, and reheating are given in Figure 3. The temperature versus swelling extension modulus (SEM) curve during reheating can also be constructed by measuring one by one the elongation and the corresponding extension force of the swelling fiber at various, approximately constant temperatures during a slow process of programmed temperature rise. The results are shown in Figure 4. Both the extension and relaxation traces appear as straight lines, from which the modulus can be calculated.

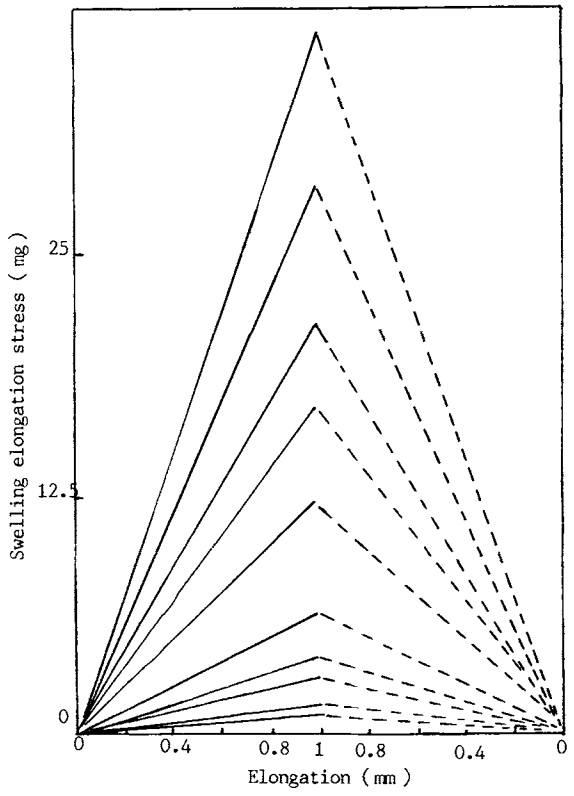

Figure 4(a) Extension and retraction lines measured at various temperatures during the reheating process ('fed') as described in Figure 3 (sample: single filament of 2.56 dtex resulting from Fig. 3).

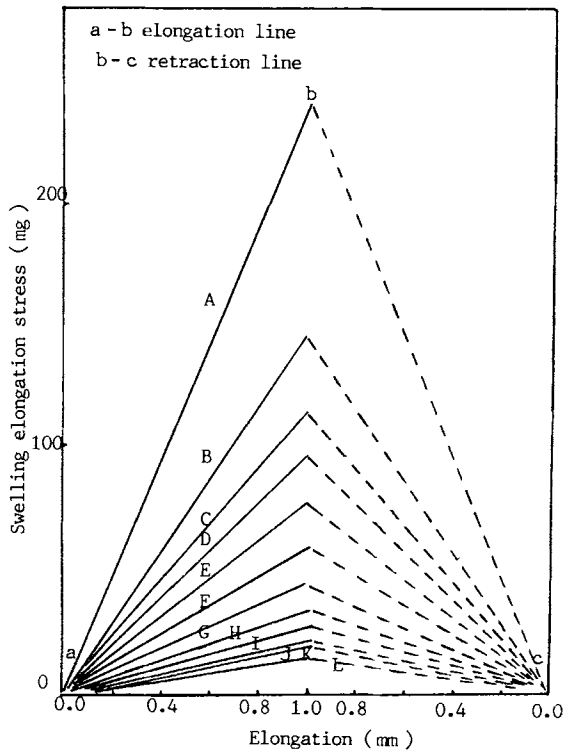

Figure 4(b) Same as Figure 4(a), UHMWPAC fiber.

A typical temperature versus swelling extension modulus curve of a PAC fiber sample measured as described above is shown in Figure 5(a). The modulus of the fiber at the terminal stage is termed the terminal swelling extension modulus (TSEM). This stage cannot be kept very long; the fiber will be dissolved very soon during temperature rise. At the terminal stage, the curve will appear as a short, relatively flat portion. Figure 5(b) is a similar temperature–modulus curve for an UHMWPAN fiber. It will be further discussed that the terminal swelling extension modulus is a unique property of the entanglement loopings of the swelling fiber sample.

Preparation of a Series of Model Acrylic Fibers for Systematic Study of Effect of Shearing on Entanglements

For this purpose, a simple apparatus was designed and constructed, as shown in Figure 6. In essence,

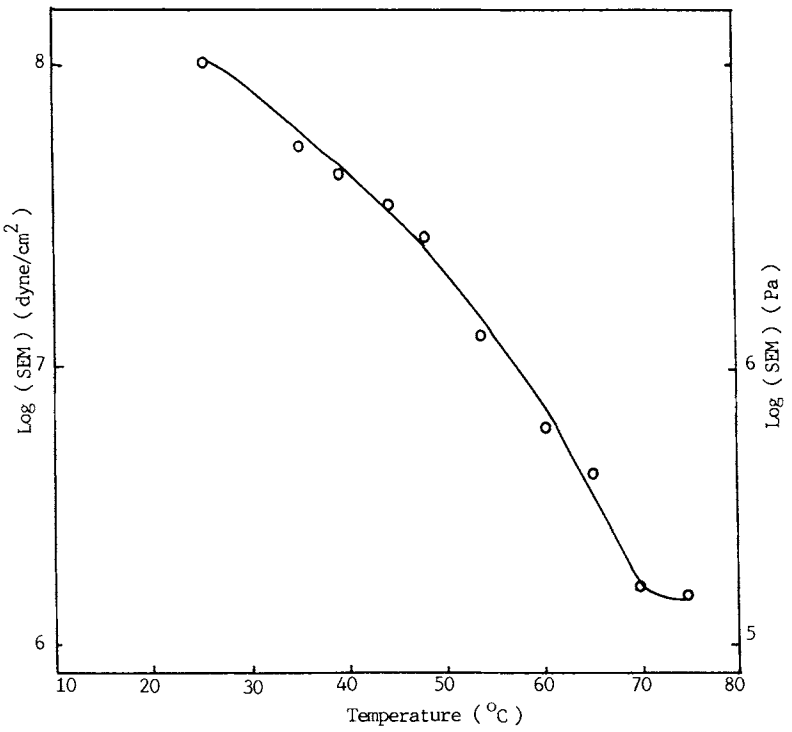

Figure 5(a) Temperature–swelling extension modulus (SEM) curve calculated from Figure 4(a) of a PAC fiber.

it is just a capillary rheometer with an attachment for measuring the die swell added. A schematic diagram of the die swell is shown in Figure 7. A series of die swell photos for spinning UHMWPAC model fibers with different aspect ratios (L/D) are shown in Figure 8.

For most of the model fibers prepared, the volumetric throughput of the spinning solution into spinning jets was kept constant, that is, the shear rate for flow in the spinning capillaries was constant. A set of spinning jets of different aspect ratios $L/D = 2, 4, 6, 8, 10$, and 15 were employed; the diameter (D) of all spinning jets used was 0.8 mm. With a definite diameter of spinning jets and constant throughput the shear rate was fixed, but the time of stay in the capillary increased with increasing capillary aspect ratios of the jets employed.

Other parameters that can be varied during the model fiber spinning are volumetric throughput (Q), which results in various shear rates of flow in the capillary, and the molecular weight of the acrylic polymer employed. These tend to modify the entanglement of the model fiber produced.

The model fiber samples so produced were subjected to a moderate degree of drawing of 4 times in order to stabilize their texture, better suited for testing later.

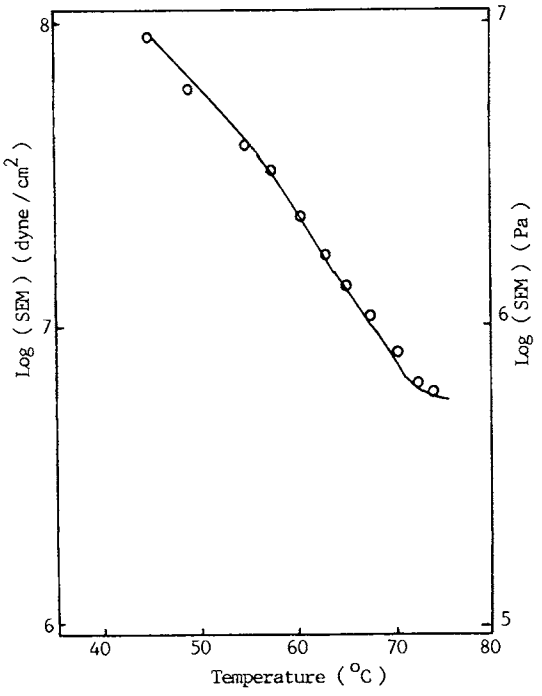

Figure 5(b) Temperature–swelling extension modulus (SEM) curve of an UHMWPAC fiber, calculated from Figure 4(b).

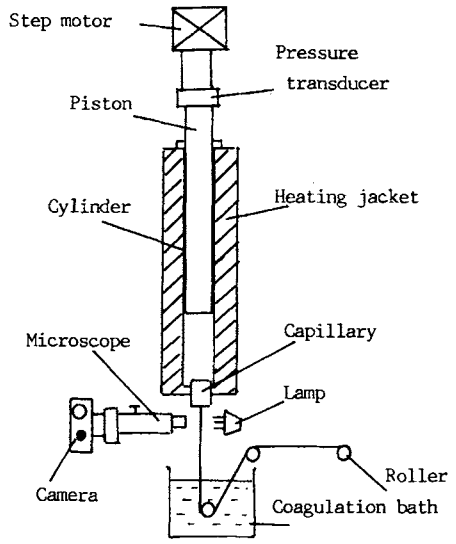

Figure 6 An apparatus for preparing model acrylic fibers under various conditions.

Tests of Model Acrylic Fibers for Entanglement Study

With the fiber samples produced above, we would be able to measure the entanglements present in the sample by three thermal methods, the TSEM, the swelling differential scanning caloriemetry (SDSC), and the ratio of SSS to SS, designated as SSS/SS or R test. These results were then checked by that of die swell. All results are described in detail below.

Temperature Versus SEM Curves

In Figures 9(a,b) the temperature versus SEM curves of model PAC fibers of ordinary molecular weight, 6×10^4 and UHMW, 71.2×10^4 prepared with capillaries of various aspect ratios (L/D) are shown. The effect of increasing aspect ratios is a general lowering of moduli of the swelling fiber, certainly due to disentanglements through shear. For other details, see the illustration of Figure 9.

The effects of the molecular weight in a certain range on the temperature versus SEM curves of model PAC fibers are shown in Figure 10. The influences of the shear rate (ranging from 243 to 1460 s^{-1} via changing the volumetric throughput during spinning) on the temperature versus SEM curves of model PAC fibers are shown in Figure 11. For all other details, see the illustrations of these figures.

SDSC Records of PAC Fibers and Measurement of Entanglement Energy (Q_e)

In Figure 12(a,b), we show the SDSC records of the same model PAC fibers as used in Figure 9(a) (with shear rate 970 s^{-1} and L/D as a parameter) and as used in Figure 11 (with $\dot{\gamma}$ as a parameter), respectively. From the entanglement peak of these SDSC records the entanglement energy (Q_e) of these fiber samples prepared under various conditions can be measured, as described in a previous publication.[5] The results are given in Tables 1 and 2. The significance of these results will be further explained in the Discussion section.

Reading of TSEM from Temperature–Swelling Extension Modulus Curves

From the temperature versus SEM curves of Figures 9–11, we can easily derive the TSEM values of the corresponding samples. On the other hand, according to the classical theory of rubber elasticity,[6] the extension modulus of a rubber macromolecular network system can be calculated by the equation

$$E = 3\rho RTN \tag{1}$$

in which E is the extension modulus, ρ is the density of the dry fiber, R is the gas constant, T is the absolute temperature, and N is the number of cross-linked chains/mol of material. For a swelling model PAC fiber, the applicability of this equation for calculating the number of entangled segments depends upon the rubber-like character of the swelling fiber in which the macromolecular looping entanglements act as cross-links of the network, which we have thoroughly proved before. Thus, from TSEM values, the number of entanglements (N_e) present in the terminal swelling state of the corresponding model

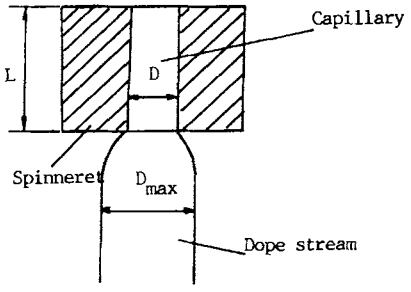

Figure 7 Typical die swell diagram. Die swell ratio = D_{max}/D. Capillary aspect ratio = L/D.

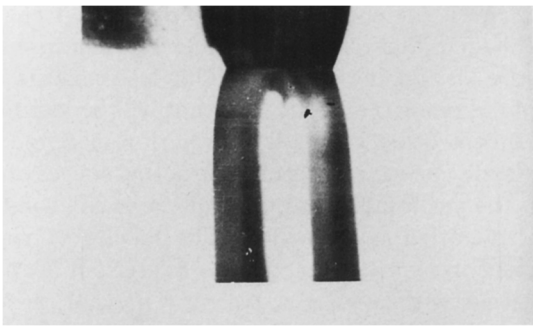

(a). L/D= 2; Die Swell Ratio=1.36

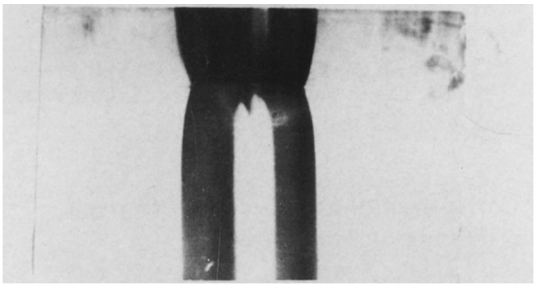

(b). L/D=4; Die Swell Ratio=1.33

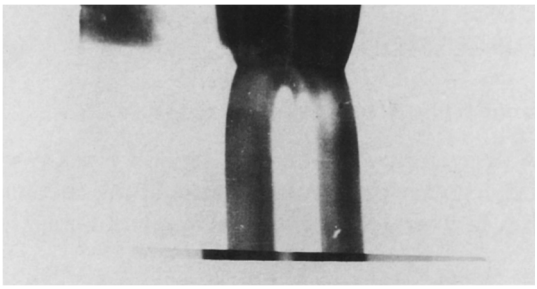

(c). L/D=6; Die Swell Ratio=1.29

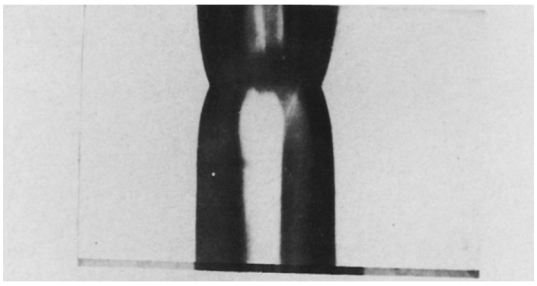

(d). L/D=8; Die Swell Ratio=1.27

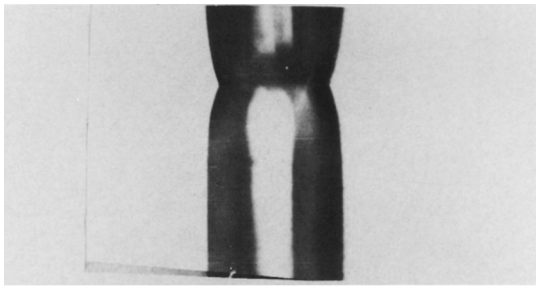

(e). L/D=10; Die Swell Ratio=1.24

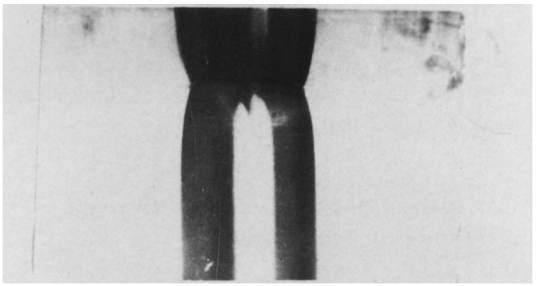

(f). L/D=15; Die Swell Ratio=1.21

Figure 8 An assembly of die swell photos with six different aspect ratios.

PAC fibers can be calculated by eq. (1). For simplicity, in this calculation we have made several approximations: identifying the number of entangled segments with entanglements; neglecting a term for correction of the effect of swelling on the modulus that can be done by multiplication of the right-hand side by a correction factor $V_r^{1/3}$ where V_r is the ratio of unswollen volume to the swollen one.[6] For comparative purposes when the solvent is fixed, approximations are justifiable.

The value of $V_r^{1/3}$ for a PAC fiber can be determined from a thermal swelling micrograph of such a fiber[5a] as roughly 0.6.

Furthermore, from the SDSC results concerning the entanglement energy Q_e of the corresponding samples and the number of entanglements (N_e) just obtained, we can calculate the amount of energy per unit entanglement (E_e). These are tabulated in Tables 1 and 2.

Typical SSS and SS of PAC Model Fibers

This is shown in Figure 1(a,b) for a sample of UHMWPAN fibers. Data for fibers of different M_w and SSS/SS ($=R$) are listed in Tables 3–5.

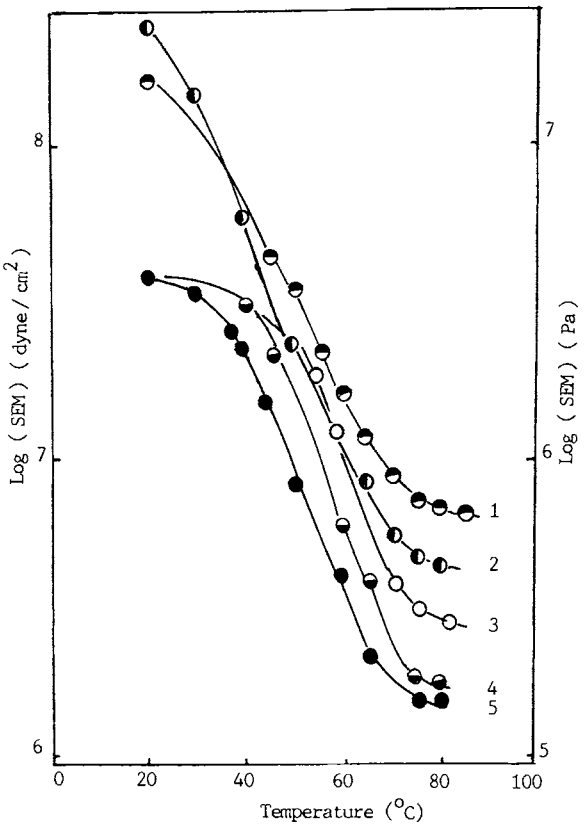

Figure 9(a) Temperature versus swelling extension modulus (SEM) curves of PAC fibers with L/D as parameter ($\bar{M}_w = 6 \times 10^4$; 8.1% MA; 25% dope concentration; D = 0.8 mm; shear rate ($\dot{\gamma}$) = 970 s^{-1}; draw ratio = 4). L/D: 1, 4; 2, 6; 3, 8; 4, 10; 5, 15.

Further Correlation of Measured and Derived Results of Testing on Model Fibers

In Figure 13, we show the effects of the capillary aspect ratios on the measured die swell ratios during spinning of PAC model fibers with molecular weights as parameters.

The effects of the capillary aspect ratios during spinning of PAC model fiber of $\bar{M}_w = 6 \times 10^4$ and 71.2×10^4, on the measured values of R, Q_e, log(TSEM), and die swell ratio, are shown in Figure 14(a) and (b), respectively.

The effects of shear rates ($\log \dot{\gamma}$) during spinning on the measured values of Q_e, R, and log(TSEM) are shown in Figure 15.

The effects of molecular weight on the measured value of R, die swell ratio, and log(TSEM) are shown in Figure 16.

The significance of these experimental results given above will be further discussed in the following section.

With the apparatus for model fiber preparation shown in Figure 6, it is possible to measure the pressure loss during spinning. This loss consists of two parts, one is a viscous part that will be lost forever, and the other is elastic energy that is stored in the elastic network structure, the actual source of which is the macromolecular entanglements. Theoretically, it is rather complicated. The results of viscosity measurements will appear in a later publication together with results concerning normal stress and die swell. Rheological methods of studying entanglements are well represented in the literature.[7]

DISCUSSION

Bond Theory of a Polymer Fiber Texture

A practically valuable polymer fiber possesses certain specific properties because of the chemical and physical structure of the macromolecular aggregates.

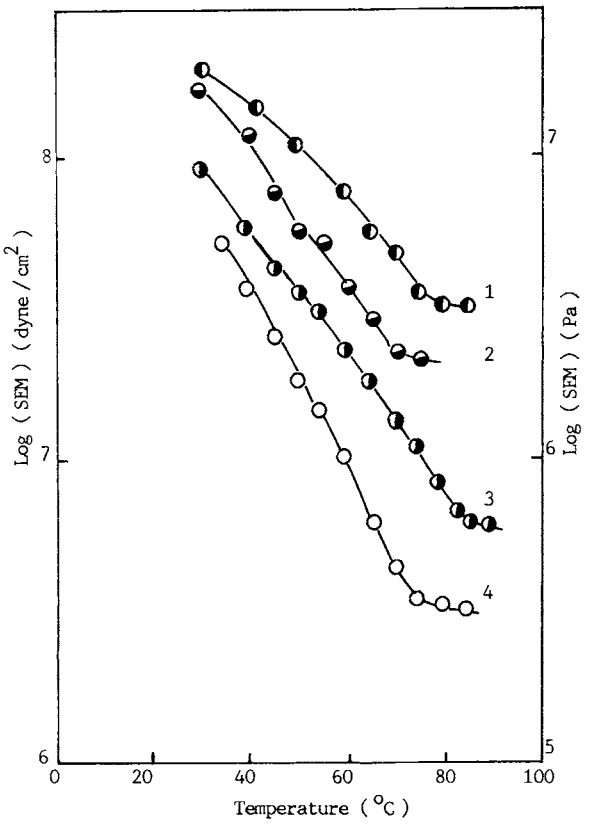

Figure 9(b) Temperature versus swelling extension modulus (SEM) curves of PAC fibers with L/D as parameter ($\bar{M}_w = 71.2 \times 10^4$; 8% dope; D = 0.8 mm; $\dot{\gamma}$ = 485 s^{-1}; draw ratio = 4). L/D: 1, 4; 2, 6; 3, 8; 4, 10.

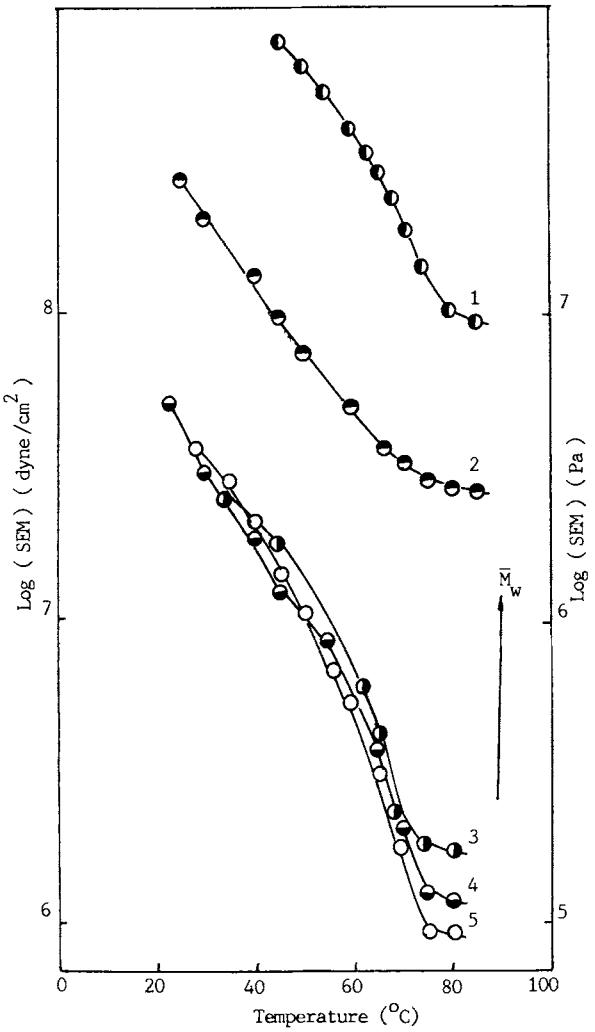

Figure 10 Temperature versus swelling extension modulus (SEM) curves of PAC fibers with $\bar{M}_w$ as parameter (10% MA; 8% dope; L/D = 15; D = 0.8 mm; $\dot{\gamma}$ = 485 s^{-1}) $\bar{M}_w \times 10^{-4}$: 1, 97.1; 2, 71.2; 3, 53.6; 4, 42.5; 5, 33.4.

The macromolecules are bonded together in a more or less ordered way, designated as the super-molecular structure or texture of the fiber. In a semicrystalline fiber, the least ordered region is the amorphous one; the average bond energy density here is the lowest, and regularity of bonds is poor. However it is in this region where the macromolecular entanglements are expected to be concentrated. In the crystalline region, a lattice structure of different degrees of crystalline regularity and crystallite size exists. In an SDSC thermogram the sequence of occurrence of the amorphous peak and the crystalline peak is in general the same as their bond energy density. The energy in conjunction with the small protrusion peak at the latter portion of the SDSC thermogram is termed the entanglement energy. Actually, the amount of energy due to the entanglement looping itself is quite small; most of the energy related to the protrusion peak is due to the couplings between the macromolecular segments in the neighborhood of the loopings.[3]

The entanglement energy peak[5] usually appears at the latter portion of the SDSC thermogram. With increasing molecular weights, both the crystalline peak and the entanglement peak will shift toward the high temperature side, but the former will shift at a much higher rate then the latter. Hence, with UHMWPAN and UHMWPAC fibers, the entanglement peak will coincide with the crystalline peak and hence become indistinct and cannot be employed for studying entanglement. Therefore, no data of the entanglement energy were given

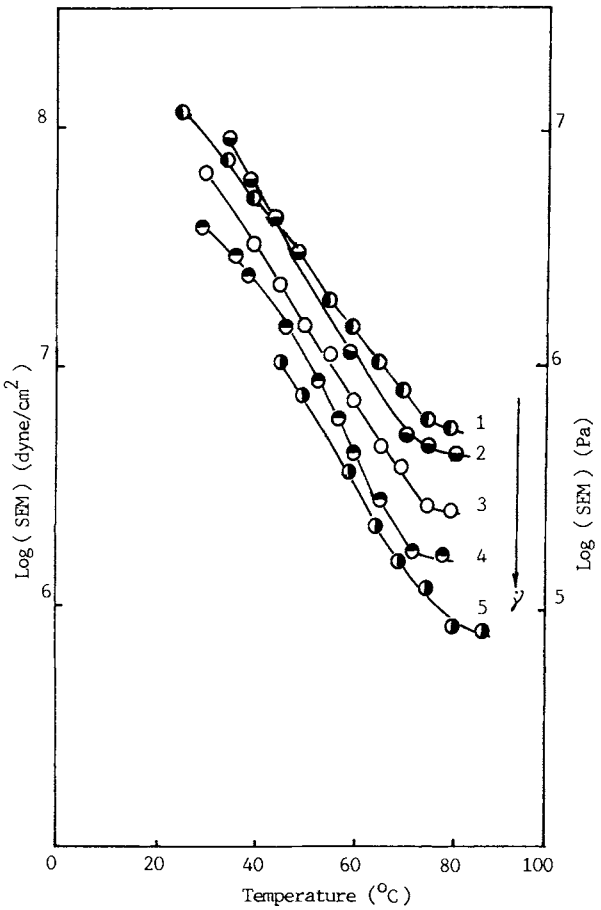

Figure 11 Temperature versus log(SEM) curve of PAC model fibers with $\dot{\gamma}$ as parameter ($\bar{M}_w$ = 6 × 10^4; 8.1% MA; 25% dope; L/D = 15; D = 0.8 mm; draw ratio = 4). $\dot{\gamma}$ (s^{-1}): 1, 243; 2, 485; 3, 728; 4, 970; 5, 1460.

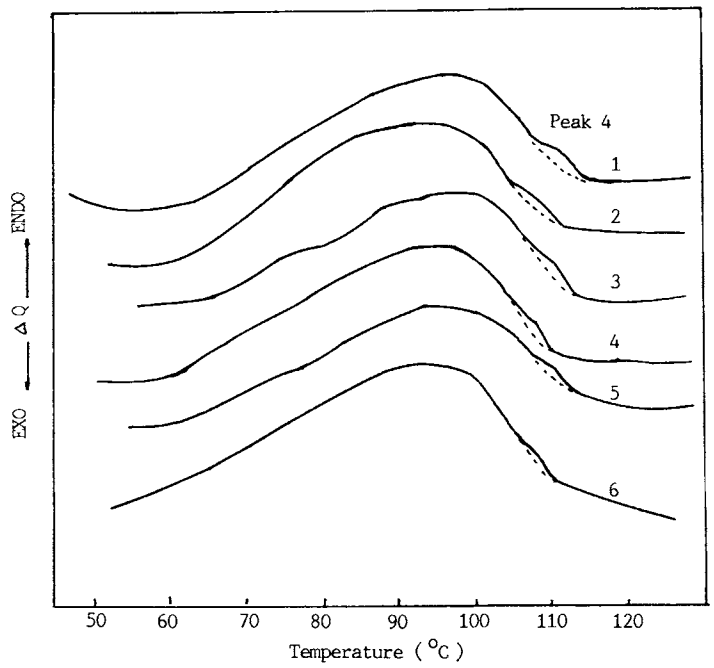

Figure 12(a) SDSC records of model PAC fibers ($\bar{M}_w = 6 \times 10^4$; 8.1% MA; 25% dope; D = 0.8 mm; $\dot{\gamma}$ = 970 s^{-1}; draw ratio = 4) with L/D as parameter. L/D: 1, 2; 2, 4; 3, 6; 4, 8; 5, 10; 6, 15.

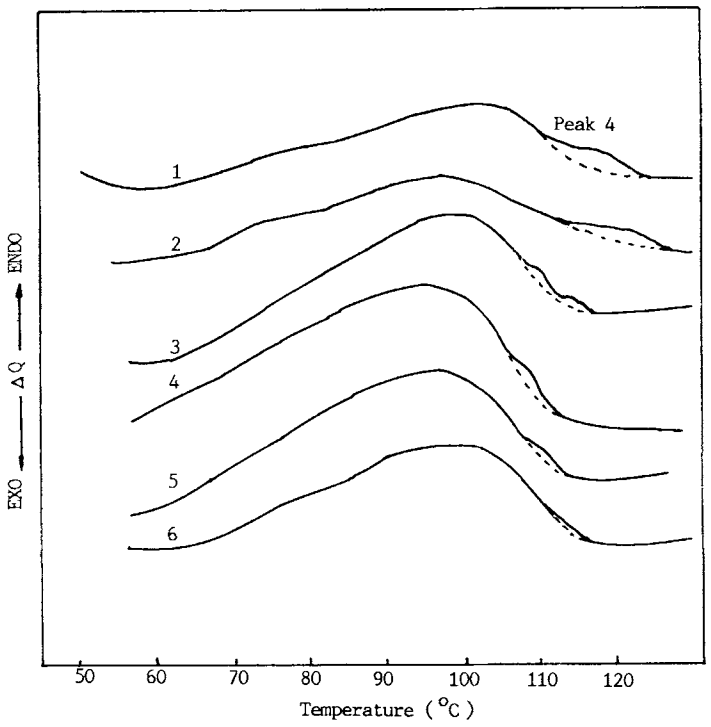

Figure 12(b) SDSC records of model PAC fibers ($\bar{M}_w = 6 \times 10^4$; 8.1% MA; 25% dope; D = 0.8 mm; L/D = 15; draw ratio = 4) with $\dot{\gamma}$ as parameter. $\dot{\gamma}$ (s^{-1}): 1, 243; 2, 485; 3, 728; 4, 970; 5, 1460; 6, 1940.

Table I Coupling Energy/Entanglement Segment (E_e) of PAC Fibers Versus Shear Rate

$\dot{\gamma}$ (s^{-1})	243	485	728	970	1460
$N_e \times 10^5$ (mol/g)	5.60	4.95	2.60	1.66	0.93
Q_e (J/g)	0.659	0.598	0.315	0.203	0.114
E_e (kJ/mol)	11.8	12.1	12.1	12.2	12.3

$\bar{M}_w = 6 \times 10^4$; 8.1% MA; 25% dope concentration; $L/D = 15$; $D = 0.8$ mm.

for UHMWPAN fibers. With UHMWPAN or UHMWPAC fibers of molecular weight over 120 $\times 10^4$, the entanglement peak might log behind so much that it might even to the low temperature side of the crystalline peak. The reversal of sequence here is actually due to the advancing of the crystalline peak because of the very high molecular weight and hence high crystallinity and very large crystallite size of the fiber sample. These phenomena are still under investigation.

From the thermomechanical behavior of the acrylic fibers as shown in Figures 1(b) and 2(c), the bond structure of the fiber can be clearly understood. Referring to the SSS curve [Fig. 1(b)], the slope shown by the initial portion of the curve is approximately constant. At a certain point a, the linearity of the curve no longer exists, and SSS already generated shows a relaxation of increasing rate until the top point b of the SSS curve is reached. a marks the beginning point where the material changes from glassy to leathery: a–b corresponds to the so-called leathery region. b–c corresponds to the crystalline plateau; c marks the beginning of dissolution of the crystalline region, and d marks the end of the same region. From d on, only macromolecular chain loopings are exerting their influences; the entanglement plateau is incomplete. In Figure 2(c) the temperature–SSM curve is similarly divided into regions like that in Figure 1(b) (the temperature–SSS curve).

The total intermolecular bond energy of a typical commercial PAC fiber when measured by DSC under swelling conditions in 80% aqueous DMF is 54 kcal/mol and 35 kcal/mol when measured dry. The difference of 19 kcal/mol is due to the heat of solvation.[4]

We may look upon the entanglement looping existing in the macromolecular networks also as a bond system whose energy measured by SDSC will vary a great deal due to different degrees of coupling of the entangled parts.[3] Although the energy involved in a topological looping itself is rather small, in comparison with that of a molecular coupling between chains the bond coupling energy formed between two neighboring, rapidly moving chain segments would certainly be influenced by the limitations imposed by loopings. Couplings between interaction groups could be formed with greater probability, thus causing additional coupling energy to arise. Samples of PAC fibers stored under ambient temperature may have their SDSC entanglement bond energy increased by several times, due to the growth of coupling energy between the neighboring chains radiating from the looping. The dual nature of the entanglement bond energy was fully ellucidated previously.[3]

Preliminary Heating of PAC Fiber Sample for Determination of TSEM

Referring to Figure 3, it can be seen that the shrinking stress of an ordinary molecular weight PAC fiber sample passes through the cycle oabcd just like that of an UHMWPAN fiber shown in Figure 1(b), although the shape of the shrinking stress segment is different in the degree of relaxation.

At the point c, nearly all the crystalline texture begins to dissociate. Further dissociation of crystalline bonds will cause a very rapid relaxation of shrinking stress already generated as shown by the shrinking stress curve segment cd. At the terminal point d, the texture is very nearly a true rubber con-

Table II Coupling Energy/Entanglement Segment (E_e) of PAC Fibers Versus Capillary Aspect Ratio

L/D	4	6	8	10	15
$N_e \times 10^5$ (mol/g)	7.33	4.39	3.14	1.93	1.66
Q_e (J/g)	0.427	0.287	0.251	0.231	0.204
E_e (kJ/mol)	5.83	6.54	7.99	11.9	12.2

$\bar{M}_w = 6 \times 10^4$; 8.1% MA; 25% dope concentration; $\dot{\gamma} = 970\ s^{-1}$; $D = 0.8$ mm.

Table III Swell Shrinking Stress (SSS) and Swell Shrinkage (SS) of PAC Fibers Prepared Under Various Capillary Aspect Ratios (L/D)

L/D	2	6	10	15
Denier (d)	33.5	45.3	53.6	46.9
SSS (mg/d)	55.2	61.8	65.3	87.4
SS (%)	8.0	10.0	13.0	24.0
R = SSS/SS	6.9	6.2	5.0	3.6

$\bar{M}_w = 6 \times 10^4$; 8.1% MA; 25% dope concentration; $\dot{\gamma} = 970$ s^{-1}; draw ratio = 4.

Table V Swell Shrinking Stress (SSS) and Swell Shrinkage (SS) of PAC Fibers with $\bar{M}_w$ as Parameter

$\bar{M}_w \times 10^{-4}$	97.1	71.2	53.6	42.5	33.4
Denier (d)	37.6	36.8	42.0	39.2	39.2
SSS (mg/d)	356.4	290.8	182.1	125.0	96.9
SS (%)	38.0	35.0	28.0	21.0	17.0
R = SSS/SS	9.4	8.3	6.5	6.0	5.7

8% dope in aqueous DMF, $\dot{\gamma} = 495$ s^{-1}, 10% MA, $L/D = 15$, $D = 0.8$ mm, draw ratio = 4.

sisted of a network of entanglement loopings only. Further heating above the point d will certainly cause the dissolution of the swollen fiber; therefore we stop the process of heating and cool the sample down slowly. The shrinking stress will lower nearly linearly and thermodynamically like a rubber[6] until the point e representing minimum shrinking stress is reached. The section of shrinking stress curve is quite linear with a positive derivative with respect to temperature until proximity to the point e is approaching. This is a characteristic of a rubber. Further cooling will probably result in a structure with dense coupling bonds, slight temperature coefficient of expansion, and rather high extension modulus. The shrinking stress of the sample increases only very slowly from e to f, evidently due to the linear thermal contraction upon cooling.

When the sample is reheated from the state at f, the shrinking stress grows up again along the path "fed," very nearly in coincidence with the original cooling path; the heating and cooling processes are approximately reversible. Through the reversible cooling and reheating process, we believe that any crystalline textural unit might have been completely eliminated and the texture consists of a network with no textural units except entanglements. Therefore, the swollen fiber is actually at the terminal swelling state, suitable for determination of TSEM and calculation of the number of entanglement loopings (N_e).

The complete temperature–swelling extension modulus curve of the heat-treated PAC fiber samples shown in Figure 5(a,b) reveal no crystalline texture. Up to 70°C, the temperature modulus curves are continuous without any break except the ending short flat portions. These are believed to be due to entanglements. The difference between Figure 5(a) and (b) is the molecular weight, (a) ordinary low molecular weight and (b) UHMW resulting in different terminal swelling modulus of approximately 2×10^5 and 7×10^5 Pa (2×10^6 and 7×10^6 dyne/

Table IV Swell Shrinking Stress (SSS) and Swell Shrinkage (SS) of PAC Fibers Prepared Under Various Shear Rates

$\dot{\gamma}$ (s^{-1})	243	485	728	970	1940
Denier (d)	29.7	22.2	35.9	46.9	43.4
SSS (mg/d)	84.2	121.6	86.4	87.4	117.5
SS (%)	12.0	18.0	20.0	24.0	35.0
R = SSS/SS	7.0	6.7	4.3	3.6	3.4

$\bar{M}_w = 6 \times 10^4$; 8.1% MA; 25% dope concentration; $L/D = 15$; $D = 0.8$ mm; draw ratio = 4.

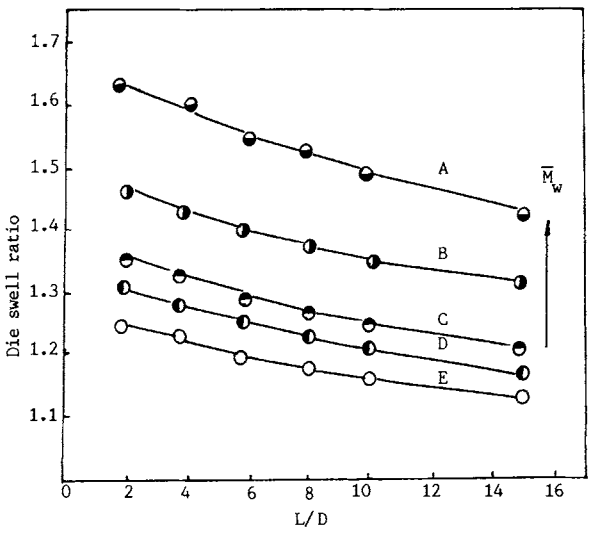

Figure 13 Effects of capillary aspect ratio (L/D) on the die swell ratio with $\bar{M}_w$ as parameter; 8% PAN dope in DMF; $\dot{\gamma} = 485$ s^{-1}; $D = 0.8$ mm. $\bar{M}_w \times 10^{-4}$: (A) 97.1; (B) 71.2; (C) 53.6; (D) 42.5; (E) 33.4.

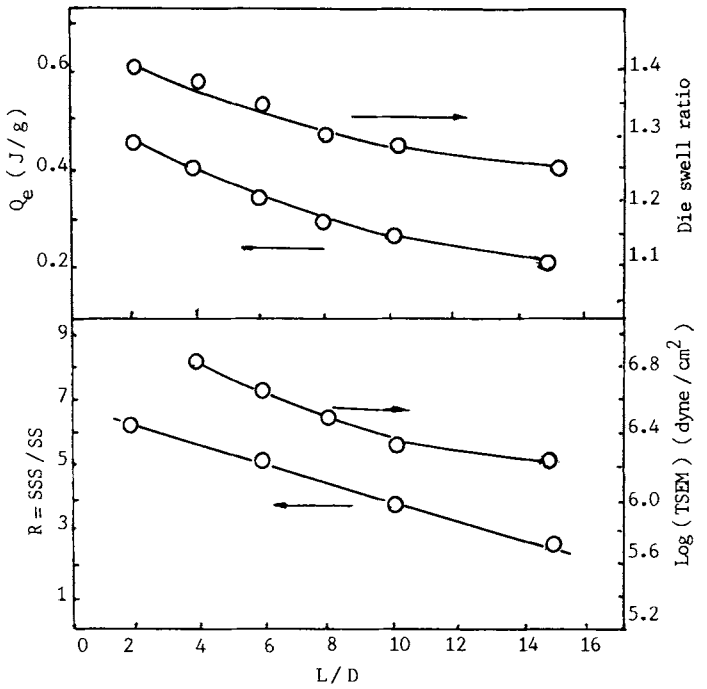

Figure 14(a) Effects of capillary aspect ratio (L/D) during spinning of model PAC fibers on the measured values of R, entanglement energy (Q_e), log(TSEM), and die swell ratio. Sample: $\bar{M}_w = 6 \times 10^4$; 8.1% MA; 25% dope; $\dot{\gamma} = 970\ s^{-1}$; $D = 0.8$ mm; draw ratio = 4.

cm^2), respectively, which indicates essentially the effect of the molecular weight on the entanglements.

Reports exist of attempted calculation of entanglements from the nonswelling plateau moduli of polymers of an amorphous structure.[8] If there are some residual crystallites in the polymer, then the result of the calculation will include the number of crystallites in the entanglement junctions.

Modification of Macromolecular Entanglements by Shearing

In polymer processing, it had long been known that shearing of a polymer melt can produce some curious effects, for example, the removal of entanglements by shearing.[9]

Similarly, the increase of loop strength of an acrylic fiber can be accomplished by mild heat treatments,[10] which are actually a process of disentanglement through the release of the frozen internal stress.[5] The true reasons for these effects was fully understood before the subject of macromolecular entanglements was taken up for detailed study. Many cases of capillary shear to modify the flow properties of polymer melts or concentrated solutions are reported as shear modification[9] that in principle are but the partial removal of entanglements in the macromolecular chain networks.

Figure 9(a,b) shows the shift of the temperature–

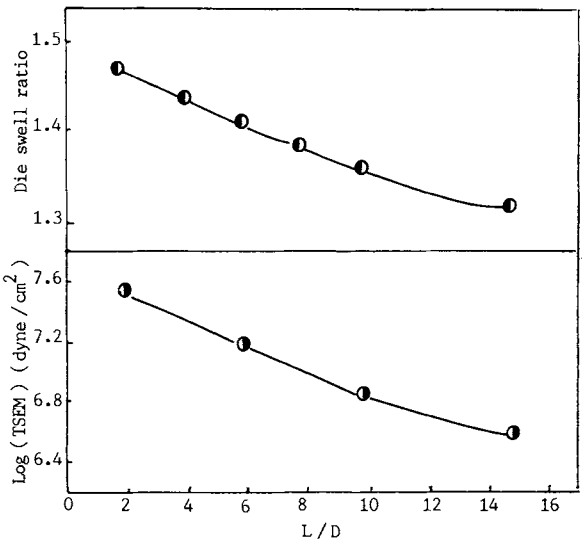

Figure 14(b) Effects of capillary aspect ratio (L/D) during spinning of model UHMWPAC fibers on die swell and log(TSEM). Sample: $\bar{M}_w = 71.2 \times 10^4$; 10% MA; 8% dope; $\dot{\gamma} = 485\ s^{-1}$; $D = 0.8$ mm; draw ratio = 4.

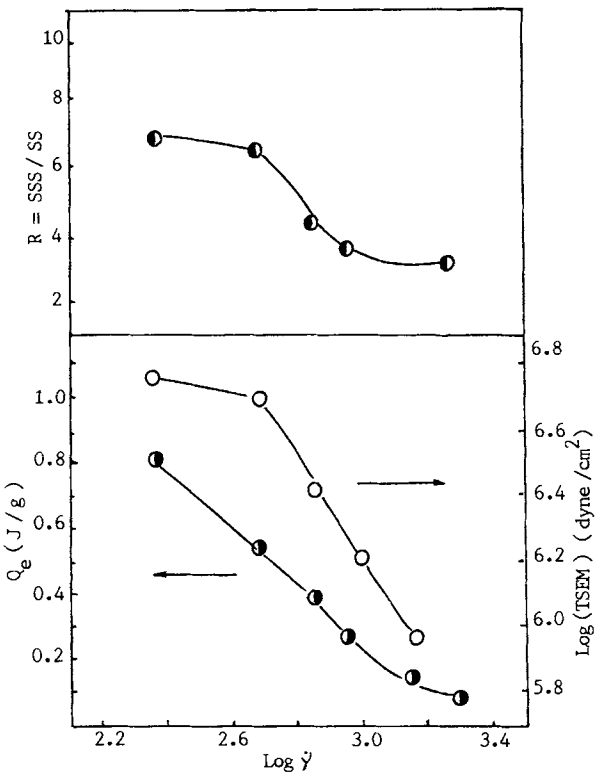

Figure 15 Effects of log $\dot{\gamma}$ on entanglement energy (Q_e), R and log(TSEM), fiber sample, same as Figure 14(a).

SEM curves of acrylic model fibers from a higher value to a lower value as L/D values are increased by steps, ordinary molecular weight usually used in commercial Jinglun fibers and UHMW prepared in our laboratory by a process termed gel spinning. The lowering of SEM, that is, disentanglement, with increasing L/D for both fibers is obvious. For other details, see the respective figure legends. The meaning of Figures 10 and 11 is similar to that of Figure 9, except the parameters used are the molecular weight and the shearing rate ($\dot{\gamma}$).

Figure 12(a,b) is the SDSC thermograms of a model PAC fiber, prepared in the laboratory, using L/D and $\dot{\gamma}$ as parameters, respectively. The area of peak 4, representing the entanglement energy,[5b] decreases with increasing L/D and increasing shear rate. The significance of these SDSC thermograms will be further expounded.

These experimental facts reflect more or less the modification of entanglements through shearing. The two terms shear modifications and macromolecular disentanglements may be viewed as equivalent. Because the elastic properties of an uncrosslinked acrylic polymer system consisting of linear macromolecular chains depends mainly on the presence of entanglements, the flow properties of acrylic polymer concentrated solutions are deeply changed by shear modifications due to the change of entanglements.

Comparison of Different Methods of Studying and Measuring Entanglements

There are two general groups of methods for studying macromolecular entanglements. The first group are the thermal methods such as the SDSC, R, and the TSEM methods; the second group are rheological methods.

Measurement of the entanglements in a polymer fiber by thermal methods depends upon the thermal effects produced on a swelling fiber. During the measurement, the fiber sample remains unimpaired. With the measurement of entanglement by rheological methods, some elastic energy must first be stored in the entangled texture by shear flow through some form of capillary space. However, this shear flow will also cause some loss of entanglement loopings. This is a contradiction that is difficult to solve.

Among the thermal methods, the TSEM method is reliable. However, most fibers consist of monomers

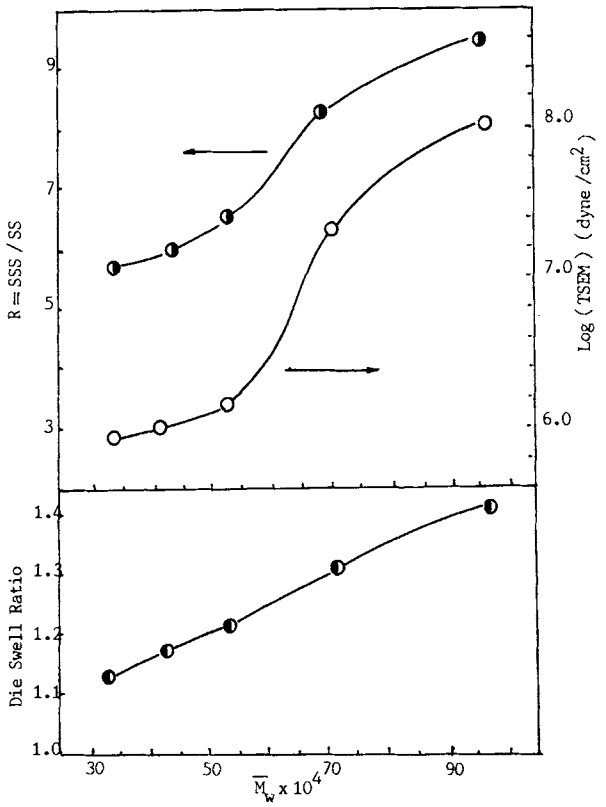

Figure 16 Effects of UHMWPAC fibers on the measured values of R, die swell ratio and log(TSEM). Sample: 10% MA; 8% dope; L/D = 15; D = 0.8 mm; $\dot{\gamma}$ = 485 s^{-1}.

with polar groups that will cause interactions between chain segments, even under the fully swollen state. This might cause the rubber equation to not fit the entanglement calculation from the TSEM of the fibers. More extensive experimental work for different individual fibers must be done before a general conclusion can be reached.

The dual coupling and looping[3] nature of the entanglement bond energy as revealed by the SDSC thermogram must be taken into careful consideration. In many cases the entanglement peak in the SDSC thermogram is only contributed by the looping entanglement. Nevertheless, fiber samples can be directly used in the DSC instrument, and results acquired quickly. It is very serviceable for comparative purposes.

The measurement of entanglements by means of R can be found in a previous article.[3]

From the Q_e values obtained in SDSC thermograms and the value of N_e calculated from TSEM, the energy per entanglement bond E_e (Q_e/N_e) can be calculated, as listed in Tables 1 and 2. It is interesting to note that when the experiment is done with $\dot{\gamma}$ as the parameter at a fixed value of L/D at 15, the E_e ($=Q_e/N_e$) value is nearly a constant around 12.1 kJ/mol. If the parameter used in the experiment is L/D, the resulting E_e values are also nearly constant (Table 2) around 12 for high L/D, but they drop a great deal for low values of L/D. As a preliminary attempt, we propose the following exposition.

During the streamline flow of a highly viscous spinning solution through a capillary, a velocity gradient exists between the liquid layer at the wall and the center of the capillary, the velocity distribution being usually parabolic. The shear produced both at the wall and at the center causes a certain amount of macromolecular disentanglements and hence a lowering of N_e values calculated. Furthermore, the shear at the wall will exert a certain peculiar frictional effect on the system of macromolecular chains. In the resulting fiber the magnitude of the Q_e values measured from the SDSC thermogram may possibly be thus enhanced just as a certain drawing of the swelling fiber would do. Therefore, as the results in Table 1 showed, where a high constant value of L/D at 15 was always used and $\dot{\gamma}$ was used as a parameter, the frictional effect of a certain shear at the wall is constant. The N_e then depends only on $\dot{\gamma}$, and the Q_e must certainly depend on N_e, so $E_e(=Q_e/N_e)$ is approximately constant at 12.1 kJ/mol whatever value $\dot{\gamma}$ may be.

For the results shown in Table 2, the parameter used was L/D ranging from 4 to 15 at a constant value of 970 s^{-1}. Lowering of L/D would cause proportionate changes in Q_e and N_e, but diminishing values of L/D would exert lower frictional effects at the wall and hence diminish $Q_e/N_e(E_e)$ from 12 to 5.8 kJ/mol.

Figures 13–16 correlate the variables L/D, $\dot{\gamma}$, and polymer $\bar{M}_w$ (each of which affects entanglements existing in the model acrylic fibers) with the polymer fluid or fiber properties, like the die swell ratio, Q_e, SSS/SS, and TSEM that represent different methods of experimental determination of entanglements.

The loss of pressure during model fiber preparation has been carefully measured; we should be able to calculate the shear stress, and with this and the shear rate to calculate further the shear viscosity of each polymer solution before coagulation. The source of die swell and normal stress is certainly due to the elastic nature of the irregular coiling conformation of the macromolecules and the entanglement loopings present in the macromolecular network texture. We prefer to leave the study of macromolecular entanglements by rheological methods to a future publication.

This work was done under the joint auspices of the National Foundation for the promotion of Natural Science and China Petrochemical Corporation.

REFERENCES

1. J. D. Ferry, *Viscoelastic Properties of Polymers,* Wiley, New York, 1980, p. 30.
2. B. Qian, H. Tian, P. Yang, and Z. Wu, *J. Eng. Industry,* **105,** 88 (1983).
3. B. Qian, P. Hu, J. He, J. Zhao, and C. Wu, *Polym. Eng. Sci.,* **32,** 1290 (1992).
4. B. Qian, J. Qin, Z. Wu, C. Wu, P. Hu, and J. Zhao, *J. Appl. Polym. Sci.,* **45,** 871 (1992).
5. B. Qian, Z. Wu, P. Hu, J. Qin, C. Wu, and J. Zhao, *J. Appl. Polym. Sci.,* (a) **42,** 1155 (1991), (b) **47,** 1881 (1993).
6. J. J. Aklonis and W. J. Macknight, *Introduction to Polymer Viscoelasticity,* Wiley, New York, 1983.
7. A. Ajji, D. J. Carreau, and H. P. Shrecber, *J. Polym. Sci. B, Polym. Phys.,* **24,** 1983 (1986).
8. S. Wu, *J. Polym. Sci. B, Polym. Phys.,* **27,** 723 (1989).
9. A. Rudin and Schreiber, *Polym. Eng. Sci.,* **23,** 422 (1983).
10. Shanghai College of Textile Technology, *The Technology and Principles of Jinglun Production,* The Shanghai Peoples Press, Shanghai, 1976 (in Chinese).

Received April 5, 1993
Accepted February 5, 1994